Available online at www.sciencedirect.com
ScienceDirect
Journal of the European Ceramic Society 27 (2007) 53–59
www.elsevier.com/locate/jeurceramsoc

Gas permeability and mechanical properties of porous alumina ceramics with unidirectionally aligned pores

Toshihiro Isobe [a], Yoshikazu Kameshima [a], Akira Nakajima [a], Kiyoshi Okada [a,*], Yuji Hotta [b]

[a] *Department of Metallurgy and Ceramics Science, Tokyo Institute of Technology, 2-12-1 O-okayama, Meguro, Tokyo 152-8552, Japan*
[b] *Advanced Manufacturing Research Institute, National Institute of Advanced Industrial Science and Technology (AIST), 2266-98 Anagahora, Shimo-Shidami, Moriyama-Ku, Nagoya 463-8560, Japan*

Received 14 October 2005; received in revised form 27 January 2006; accepted 4 February 2006
Available online 27 March 2006

Abstract

Porous alumina ceramics having unidirectionally aligned cylindrical pores were prepared by extrusion method and compared with porous ceramics having randomly distributed pores prepared by conventional method, and their gas permeability and mechanical properties were investigated. SEM micrographs of the porous alumina ceramics prepared by the extrusion method using nylon fibers as the pore former showed excellent orientation of cylindrical pores. The bending strength and Weibull modulus of the extruded porous alumina ceramics with 39% porosity were 156 MPa and 17, respectively. These mechanical properties of extruded samples were higher than those of the conventional porous alumina ceramics. The strength decreased from 156 to 106 MPa with increasing pore size from 8.5 to 38 μm. The gas permeability of the extrusion samples is higher than that of the conventional samples and increased with increasing of porosity and pore size.

Keywords: Extrusion; Fibers; Al_2O_3; Membranes; Mechanical properties; Porous ceramics

1. Introduction

Porous ceramics are used as filters, catalyst carriers or as insulators at high temperatures. Recently, applications for separation filters have become important to reduce environmental pollution in various fields. One of the most important properties of porous ceramics for filters is permeability because this property directly correlates with the pressure drop during filtration. Higher permeability is thought to be obtained by controlling the microstructure, this is difficult in conventional porous ceramics because they have randomly distributed pores.[1–4] Such conventional porous ceramics require higher porosity to reach the demanded permeability,[1,5,6] and this causes lowering of the mechanical properties.[2–4,6–12] Thus, preparing porous ceramics which satisfy both high permeability and high mechanical strength is difficult by conventional porous ceramic processing. Because these properties are strongly influenced by the microstructure, controlling the microstructure of porous ceramics is essential. A promising way to satisfy both properties is thought to be realized by aligning cylindrical open pores with uniform size parallel to the flow direction. From these viewpoints, we have developed porous alumina ceramics with unidirectionally aligned cylindrical pores by an extrusion method using combustible fibers as a pore former.[13–15] The paste for the extrusion was prepared by mixing alumina powder and combustible fibers with binder and dispersant. The resulting paste was extruded and the fibers in the paste were oriented during the extrusion process, and the desired porous ceramics were obtained after the firing. For porous alumina ceramics using carbon fibers and nylon 66 fibers as the pore formers, the porosity and pore size could be changed strongly by modifying the fiber content and diameter, respectively.[14] The highly aligned cylindrical pores were also confirmed by SEM observation. The degree of pore orientation decreased with increasing fiber content. The pore size distribution measured by mercury porosimetry showed a peak at 16 μm corresponding to the diameter of the cylindrical pore and also at 4 μm corresponding to the pores formed by connecting fibers. Moreover, it was determined that optimization of the rheologi-

* Corresponding author. Tel.: +81 3 5734 2524; fax: +81 3 5734 3355.
E-mail address: kokada@ceram.titech.ac.jp (K. Okada).

0955-2219/$ – see front matter © 2006 Published by Elsevier Ltd.
doi:10.1016/j.jeurceramsoc.2006.02.030

cal properties of the paste was one of the most important factors for high fiber orientation and the microstructure with the more highly oriented cylindrical pores was obtained when the paste showed optimum rheological properties.[15] In this manner, the porous alumina ceramics with an excellent microstructure were prepared by an extrusion method using combustible fibers.

In this study, porous alumina ceramics with unidirectionally aligned cylindrical pores were prepared by an extrusion method and the effects of porosity and pore size on their permeability and mechanical properties were investigated.

2. Experimental procedure

2.1. Preparation of porous ceramics

Porous alumina ceramics with unidirectionally aligned cylindrical pores were prepared by an extrusion method using nylon 66 fibers as described in previous reports.[14,15] High purity alumina (AHP-200, Nippon Light Metal, Japan) was mixed with 0–30 vol.% nylon 66 fibers (Chubu Pile Industries, Japan) with average diameters of 9.5–43 μm and length of 800 μm. The mixture was kneaded for 1 h with 30 mass% distilled water, 4 mass% methylcellulose (SM-4000, Shin-Etsu Chemical, Japan), 8 mass% oleic acid (Wako Pure Chemical Industries, Japan) and 0.8 mass% ammonium poly-carboxylic acid (D-305, Chukyo Yushi, Japan). The paste obtained was molded using a single screw vacuum extruder (FM-20E, Miyazaki Iron Works, Japan). The paste obtained was molded using a single screw vacuum extruder (FM-20E, Miyazaki Iron Works, Japan). The dimensions of the extruder barrel and inner aperture were 20 and 5 mm Ø, respectively. The distance of convergence region and the die after convergence region were 15 and 25 mm, respectively. The breaker plate with 14 holes 4 mm Ø in diameter is installed in front the of convergence region.[14,15] The extruded green bodies were dried at room temperature for 24 h and sintered at 1500 °C for 2 h in air.

To compare, porous ceramics with random pore distribution were prepared by a conventional partial sintering method. High purity alumina powder was mixed with 0–50 vol.% poly methyl methacrylate (PMMA) (MX-1000, Soken Chemical & Engineering, Japan) spherical particle 10 μm in diameter in ethanol solvent for 30 min and the mixture was dried for 24 h at room temperature. The obtained powders were uniaxially pressed at 50 MPa for 10 min to prepare disks (20 mm Ø in diameter, 8 mm in thickness). The samples were then calcined at 600 °C for 1 h and sintered at 1500 °C for 2 h in air.

2.2. Characterization

The density and porosity of the samples were measured by the Archimedes technique using water. The microstructure of the samples was observed by scanning electron microscope (JSM-5310, JEOL, Japan). The 3-point bending strengths of the sintered samples (2 mm × 2 mm × 10 mm) were measured with a span length of 8 mm and crosshead speed of 0.5 mm/min (AGS-5kND, Shimadzu, Japan). The longest span of the samples goes to extruded direction. The average bending strength and Weibull modulus were obtained from measurements of 10 samples. The permeability of the porous ceramics was evaluated using Eq. (1):

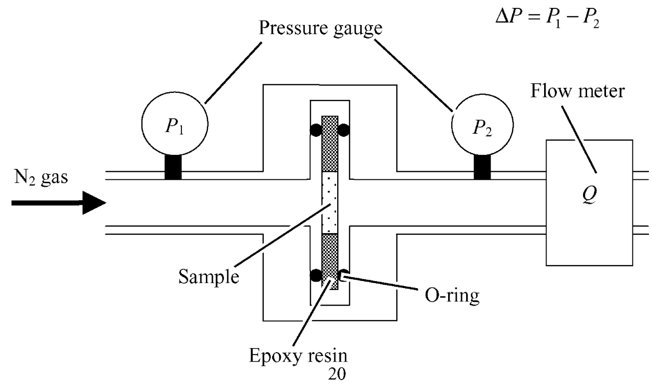

Fig. 1. Schematic model of equipment for gas permeametry.

$$\Delta P = \frac{\eta L}{\mu A} Q \tag{1}$$

where ΔP is the pressure drop from entrance to exit of the sample, μ is the Darcy's permeability, η is the dynamic viscosity of the fluid, A and L are the cross-sectional area and the thickness of the sample, Q is the flow rate. The gas permeametry equipment used in this study is shown in Fig. 1. The samples cut into 0.5–3 mm in thickness (5 mm Ø in diameter) were fixed in the center of an epoxy resin mold. ΔP and Q were measured using this equipment. The permeability is calculated from the slope of the line plotted for ΔP versus Q using Eq. (1). The dynamic viscosity η of nitrogen gas as used for the calculation is 1.75×10^{-5} Pa s.[16]

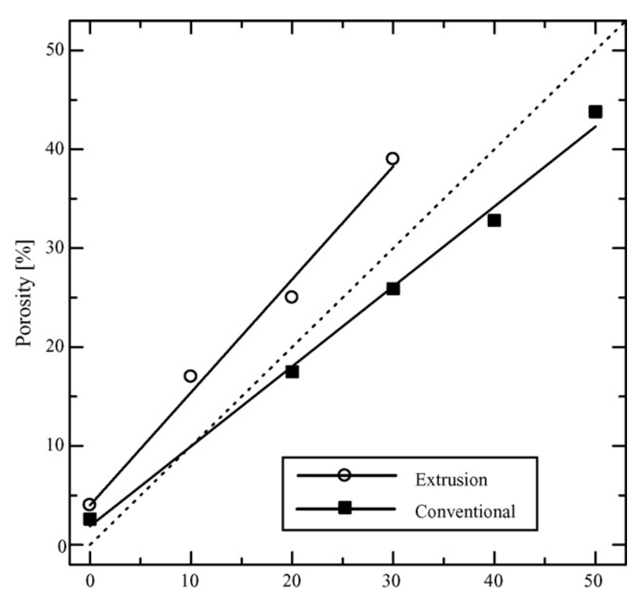

Fig. 2. Relationship between pore former content and porosity of the samples prepared by extrusion and conventional methods.

3. Results and discussion

3.1. Porosity and microstructure

Fig. 2 shows the relationship between the content of pore former and the porosity of the porous alumina ceramics. The porosities of the samples prepared without using pore formers by extrusion method and conventional method were 4 and <2%, respectively. The porosity of the samples prepared by both methods increased proportionally with increasing content of pore former. However, the increases are lower for the conventional sample than for the extruded sample, loss decrement of the voids introduced by the pore former during sintering in the second case. It is considered that nevertheless the added pore formers are mostly converted to pores after the sintering but that the extruded samples also show a residue of some small pores in the matrix.

Figs. 3 and 4 show SEM micrographs of the cross-section perpendicular and parallel to the extruded direction of the porous alumina ceramics prepared by the extrusion method. These micrographs show that cylindrical pores introduced by the pore former are highly oriented to the extruded direction. The pore shapes are shown to preserve the original fiber shape. The average pore diameters calculated by the intercept method were 8.5–38 μm and shrank about 10% from the original sizes (9.5–43 μm) during sintering. The shrinkage isotropically occurred even in the extruded samples. Fig. 5 shows SEM micrographs of the cross-section of the porous alumina ceramics prepared by the conventional method. The microstructure shows randomly dispersed spherical pores and the average pore size was 8.5 μm (the size of original pore former = 10 μm). Thus, porous alumina ceramics having the same pore size but different pore shapes are obtained and these ceramics were used for investigating the effect of pore shape on various properties.

3.2. Three-point bending strength

Fig. 6 shows the relationship between porosity and 3-point bending strength of the resulting porous alumina ceramics. The bending strengths of the dense alumina ceramics prepared by the extrusion and conventional methods were 307 (Weibull modulus of 14.0) and 356 MPa (that of 8.4), respectively. The bending strengths of the respective porous ceramics decreased to 156 (Weibull modulus of 17.4) and 69 MPa (that of 5.3) at 39 and 43% porosity, respectively. Many attempts have been reported to represent the relationship between porosity (P) and fracture strength (σ). The following general equation was proposed by Knudsen[8]:

$$\sigma = \sigma_0 \exp(-bP) \quad (2)$$

where σ_0 and b are the fracture strength at $P = 0$ and an empirical constant obtained from a slope of semi log plot, respectively.

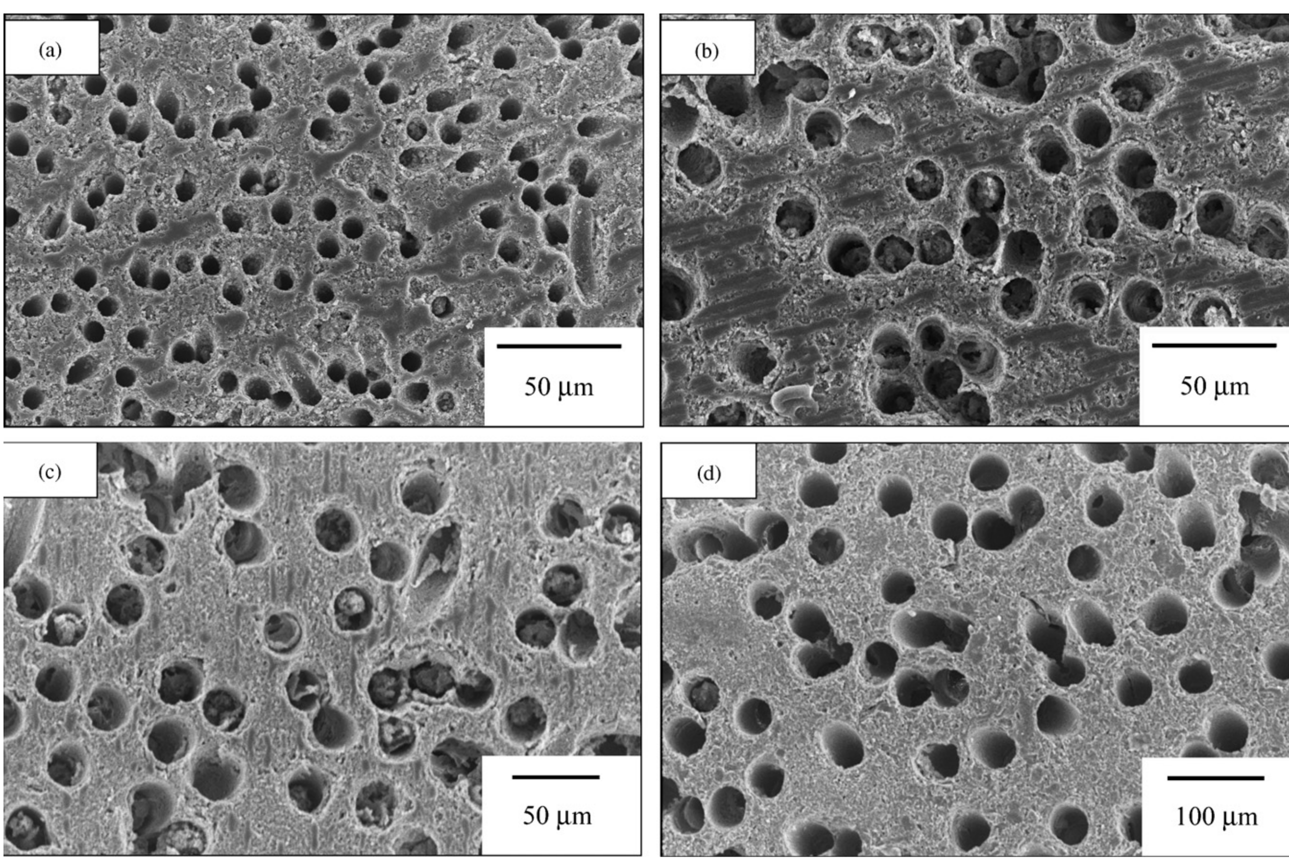

Fig. 3. SEM micrographs of cross-sections perpendicular to the extrusion of porous alumina ceramics prepared by extrusion method. The fiber contents are all 30 vol.% and fiber diameters are (a) 9.5, (b) 19, (c) 27 and (d) 43 μm.

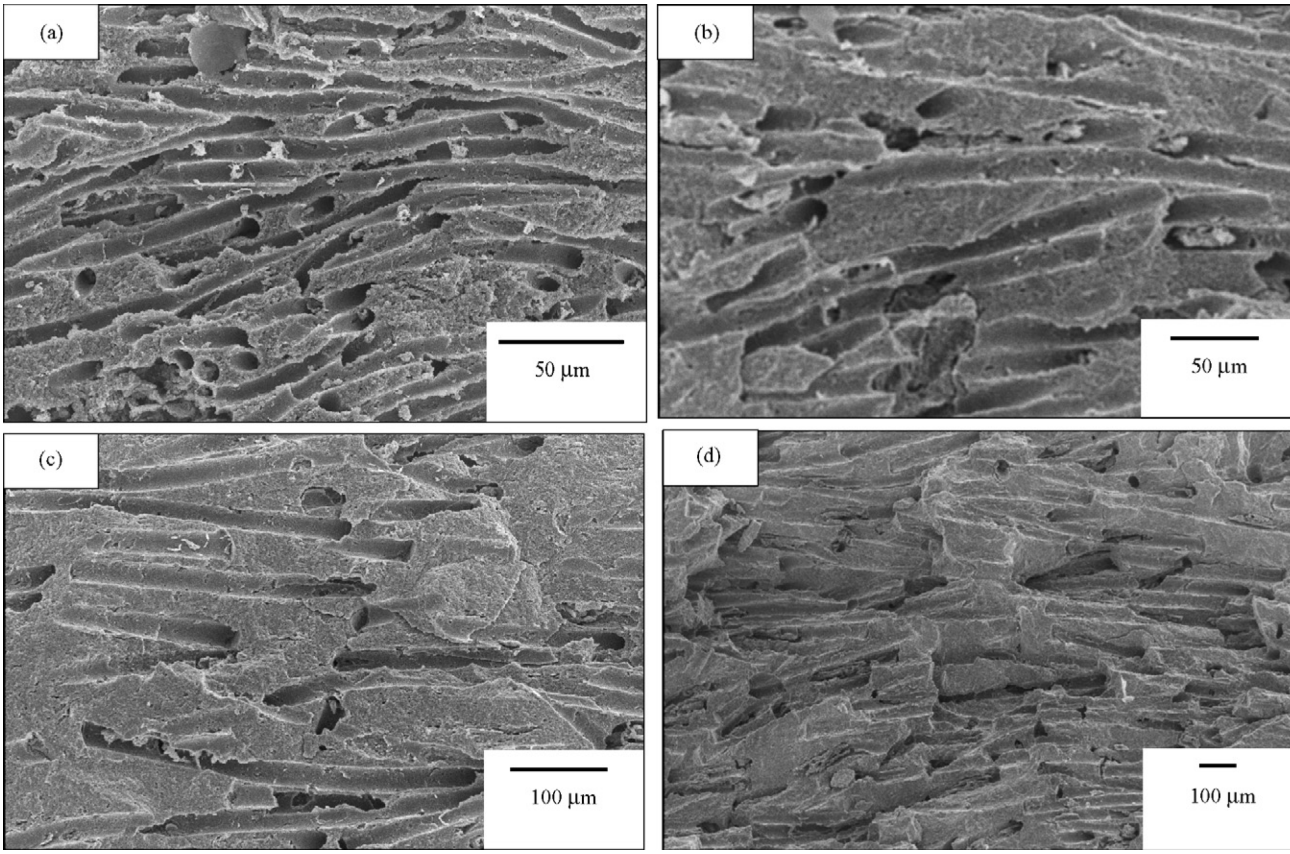

Fig. 4. SEM micrographs of cross-sections of porous alumina ceramics prepared by extrusion method parallel to the extrusion. The fiber content is 30 vol.%. The fiber content is 30 vol.%. Fiber diameters are (a) 9.5, (b) 19, (c) 27 and (d) 43 µm.

Their calculated values are listed in Table 1. The solid and broken lines in Fig. 6 are calculated from these values. The σ_0 value of the conventional sample is slightly higher than that of the extrusion sample. The b value (2.1) of the extruded sample is higher than that of the conventional sample (4.0). Thus, lowering of the strength with increasing porosity is much milder in the extruded sample than in the conventional sample and the strengths of the extruded samples become higher than the conventional samples at >7.5% porosity. It is considered that the higher bending strength of the extruded sample is attributed to the more ordered microstructure having unidirectionally aligned cylindrical pores. Porous ceramics having higher reliability are obtained by the extrusion method and it is attributed to the homogeneous microstructure.

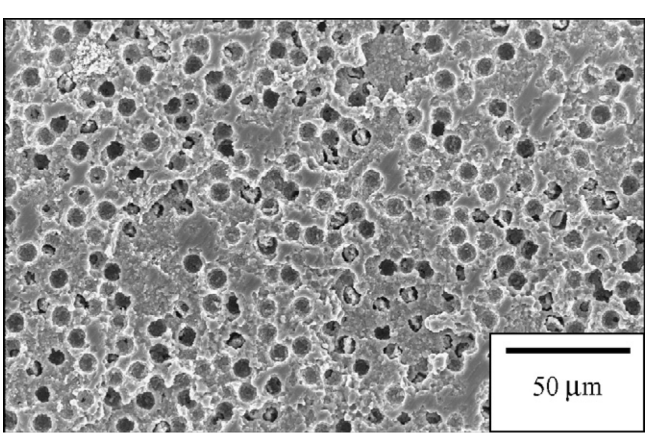

Fig. 5. SEM micrograph of cross-sections of porous alumina ceramics prepared by conventional method.

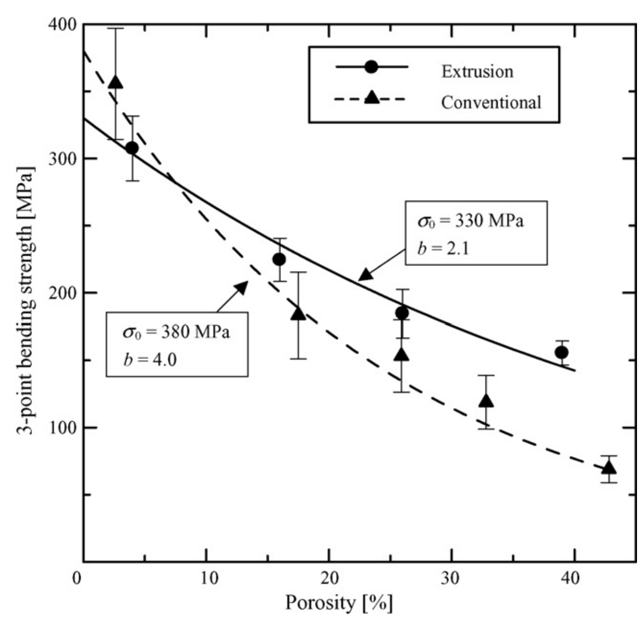

Fig. 6. Relationships between porosity and 3-point bending strength of porous ceramics prepared by extrusion and conventional methods.

Table 1
Comparison of σ_0 and b values of the porous ceramics prepared by various methods

	Material	σ_0	b
Extrusion	Alumina	330	2.1
Conventional	Alumina	380	4.0
Spriggs and Vasilos[9]	Alumina	73–574	6–8.3
Trostel[10]	Alumina		5.1
Trostel[10]	Zirconia		6.4

The b values of the present samples are compared with those prepared by partial sintering method listed in Table 1.[9,10] The reported b values ranged from 5.1 to 8.3, being slightly higher than those for the present conventional sample. The lowing of strength with increasing porosity relates not only to porosity but also to pore shape. The strength depends on the stress concentration in the vicinity of the pores (stress concentration region (σ_A)) and is given by the following equation[11]:

$$\sigma_A = \sigma\left(1 + \frac{2d_b}{d_a}\right) = K_s\sigma \tag{3}$$

where d_a and d_b are the height and width of the crack. Generally, $d_a \leq d_b$, in particular, $d_a = d_b$ for a spherical pore. The stress concentration factor (K_s) for a spherical pore is 3, which is the minimum value. Because the K_s value increases with increasing d_a/d_b values, the strength of the present conventional sample is higher than those of the reported data.

Fig. 7 shows changes of 3-point bending strength and fracture toughness of the extrusion samples as a function of pore size. With increasing pore size, the strength decreased slightly while the fracture toughness increased linearly. A relationship between pore size (d) and 3-point bending strength (σ_f) is expressed by the following equation[3]:

$$\sigma_f \propto \frac{1}{\sqrt{d}} \tag{5}$$

The strengths calculated from the Eq. (5) are shown using a dotted line in Fig. 8. The obtained strengths show good agreement with the calculated strengths. Thus, the strength drop in this sample is mainly attributed to the pore size effect.

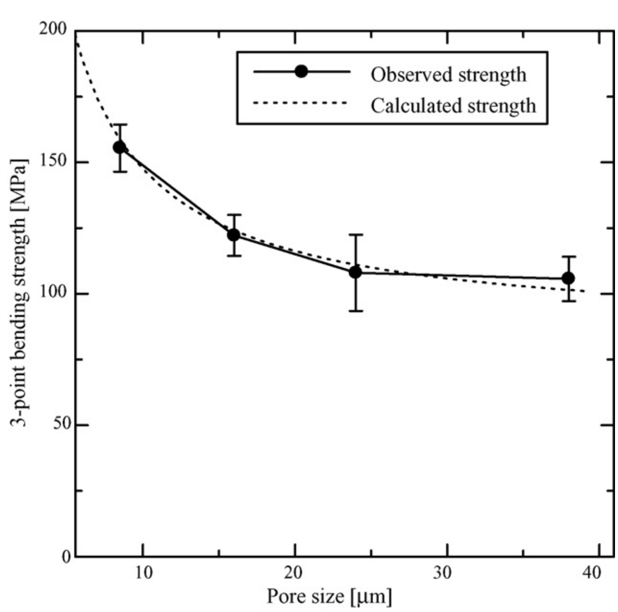

Fig. 7. Effects of pore size on 3-point bending strength of porous alumina ceramics having porosity of 39% prepared by extrusion method.

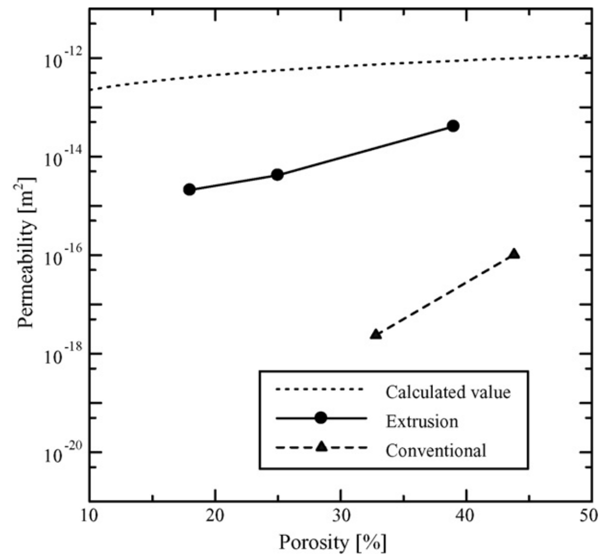

Fig. 8. Relationships between porosity and permeability of porous ceramics prepared by extrusion and conventional methods.

3.3. Gas permeability

Changes of gas permeability of the porous ceramics prepared by extrusion and conventional methods are shown in Fig. 8 as a function of porosity. For the conventional samples, permeation was not observed with a porosity of 26%, and permeation was observed with porosity of >34%, being in good agreement with the calculated porosity of >31% from the percolation model.[17] On the other hand, the extrusion samples showed permeation even with a porosity of 18%, a much lower porosity than the conventional samples. The permeability of the extrusion samples was measured with changing sample thickness from 0.5 to 3 mm but their values were almost constant irrespective to the sample thickness. The permeability of the extruded samples having 39% porosity was 4.1×10^{-14} m^2, remarkably higher than that of the conventional sample (1.0×10^{-16} m^2 at 43% porosity). Maximum permeability is obtained in an ideal model (capillary permeability model), having uniform capillary tubes aligning parallel to the gas flow direction. This permeability (μ) is calculated by the following equation[1]:

$$\mu = \frac{d^2}{32}P \tag{6}$$

where d and P are the pore size and porosity. As shown in Fig. 9, the observed permeability values of the extrusion samples are

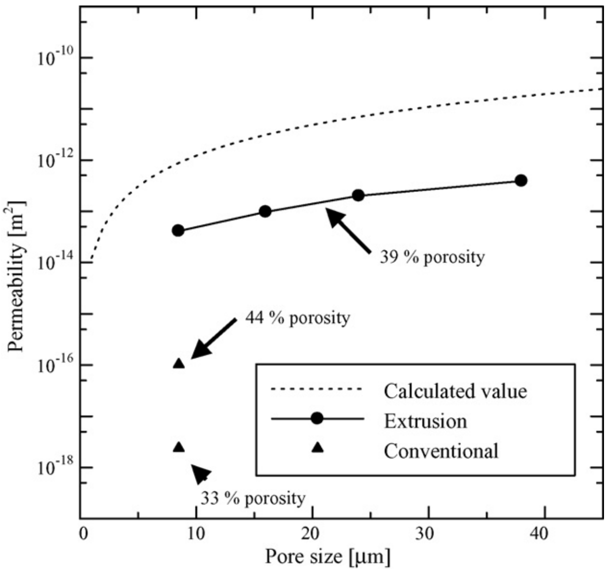

Fig. 9. Relationship between pore size and permeability of porous alumina ceramics prepared by extrusion and conventional methods.

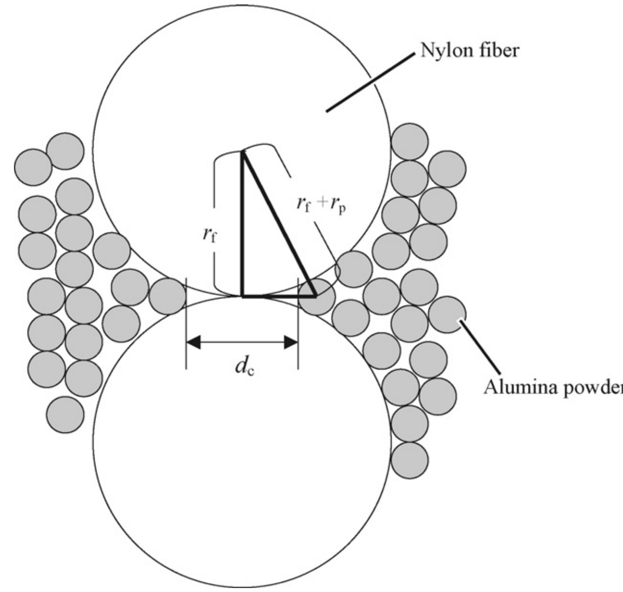

Fig. 10. Schematic model for formation of pore size (d_c) by fiber connection.

lower than the calculated ideal values. The difference becomes smaller with higher porosity of the samples. Thus, the extruded samples are seen to show excellent permeability according to the well controlled microstructure.

Fig. 9 shows relationships between pore size and permeability of the extrusion and conventional samples. The permeability calculated from the Eq. (6) is also shown in Fig. 9 by a dotted line. The permeability of the extruded samples increased slightly with increasing pore size. The observed permeability values are one to two orders lower than the calculated ideal values. This difference may be attributed to imperfections in the microstructure of the present samples. Pores in the extrusion samples are not completely straight and bent at the points connected by the contacts of original fibers. In such a case, fluid flow is thought to suffer some resistance and lowering of permeability occurs at those points. The size of the pore connection (d_c) is calculated from a model schematically depicted in Fig. 10 using the following equation:

$$d_c = 2\{((r_f + r_p)^2 - (r_f)^2)^{1/2} - r_p\} \quad (7)$$

where r_f and r_p are the radii of nylon fiber and alumina powder, respectively. The relationship between pore connection size d_c and fiber size is listed in Table 2. The calculated pore connection size is in fair agreement with the pore size measured by mercury porosimetry.[14] The permeability values calculated from Eq. (6) using these calculated pore sizes are also shown in Table 2. The calculated permeability values are in good agreement with the observed permeability values. It is, therefore, considered that the permeability of the extruded samples strongly depends on the pore connection size, corresponding to the minimum pore size in the samples.

Table 2
Calculated pore connection size and permeability of 39% porosity sample

Fiber size (μm)	d_c[a] (μm)	Permeability (m^2)	
		Observed	Calculated
9.5	2.4	4.1×10^{-14}	6.9×10^{-14}
19	3.5	9.7×10^{-14}	1.5×10^{-13}
27	4.3	2.0×10^{-13}	2.2×10^{-13}
43	5.5	3.9×10^{-13}	3.7×10^{-13}

[a] Pores formed by fiber connection.

4. Conclusions

Porous alumina ceramics with microstructures having unidirectionally aligned cylindrical pores and randomly distributed pores were prepared by extrusion and conventional methods, and their mechanical and gas permeability properties were investigated. SEM micrographs of the porous alumina ceramics prepared by the extrusion method showed excellent orientation of pores. The oriented pores were formed by burning of fiber added as pore formers only slightly shrinking after the sintering. The fracture strength of the dense alumina ceramics without using fibers prepared by the extrusion method was lower than the conventional samples (pressing method) due to the different forming processes of extrusion and conventional methods. The strength of the porous extrusion samples was 156 MPa (Weibull modulus of 17.4) at 39% porosity and higher than the conventional ceramics due to the ordered porous microstructures. The strength of the extruded samples decreased only slightly even with increasing pore size. The permeability of the extrusion samples having a pore size of 8.5 μm is 4.1×10^{-14} m^2, and is much higher than the conventional samples. The observed permeability of the extrusion samples was in better agreement with the permeability calculated from an ideal model (capillary permeability model). The porous alumina ceramics having both high strength and high permeability are achieved by controlling of the microstructure using extrusion method.

Acknowledgements

The authors thank Professor H. Awaji and Mr. S. Honda of Nagoya Institute of Technology for permitting the use of the instruments for mechanical property measurements. We also thank Professor J.S. Cross of Tokyo Institute of Technology for critical reading and editing of this manuscript.

References

1. Tomita, T., Kawasaki, S. and Okada, K., Effect of viscosity on preparation of foamed silica ceramics by a rapid gelation foaming method. *J. Porous Mater.*, 2005, **12**, 123–129.
2. Coble, R. L. and Kingery, W. D., Effect of porosity on physical properties of sintered alumina. *J. Am. Ceram. Soc.*, 1956, **39**, 377–385.
3. Ashizuka, M., Ishida, E., Matsushita, T. and Hisanaga, M., Elastic modulus, strength and fracture toughness of alumina ceramics containing pores. *J. Ceram. Soc. Japan*, 2002, **110**, 554–559.
4. Nishikawa, T., Nakashima, A., Honda, S. and Awaji, H., Effect of porosity and pore morphology on mechanical properties of porous alumina. *J. Soc. Mat. Sci. Japan*, 2001, **50**, 625–629.
5. Glass, S. J. and Green, D. J., Permeability and infiltration of partially sintered ceramics. *J. Am. Ceram. Soc.*, 1999, **82**, 2745–2752.
6. Kani, A., Osada, H., Katayama, S. and Hirabayashi, H., Gas permeability and strength of porous SiC ceramics. *J. Ceram. Soc. Japan*, 1991, **99**, 63–67.
7. Studt, P. L. and Fulrath, R. M., Mechanical properties and chemical reactivity in mullite-glass systems. *J. Am. Ceram. Soc.*, 1962, **45**, 183–188.
8. Knudsen, F. P., Dependence of mechanical strength of brittle polycrystalline specimens on porosity and grain size. *J. Am. Ceram. Soc.*, 1959, **42**, 376–387.
9. Spriggs, R. M. and Vasilos, T., Effect of grain size on transverse bend strength of alumina and magnesia. *J. Am. Ceram. Soc.*, 1963, **46**, 224–228.
10. Trostel Jr., L. J., Strength and structure of refractories as a function of pore content. *J. Am. Ceram. Soc.*, 1962, **45**, 563–564.
11. Inglis, C. E., Stress in a plate due to the presence of cracks and sharp corners. *Trans. Inst. Naval Architects*, 1913, **55**, 219–241.
12. Clobes, J. K. and Green, D. J., Validation of single-edge V-notch diametral compression fracture toughness test for porous alumina. *J. Mater. Sci.*, 2002, **37**, 2427–2434.
13. Isobe, T., Tomita, T., Kameshima, K., Nakajima, A. and Okada, K., Preparation and properties of porous alumina ceramics with oriented cylindrical pores produced by an extrusion method. *J. Eur. Ceram. Soc.*, 2006, **26**, 957–960.
14. Isobe, T., Kameshima, Y., Nakajima, A., Okada, K. and Hotta, Y., Extrusion method using nylon 66 fibers for the preparation of porous alumina ceramics with oriented pores. *J. Eur. Ceram. Soc.*, 2006, **26**, 2213–2217.
15. Isobe, T., Kameshima, Y., Nakajima, A., Okada K. and Hotta Y. Effect of dispersant on paste rheology in preparation of porous alumina with oriented pores by extrusion method, *J. Porous Mater.*, in press.
16. McCarty, R. D., Haynes, W. M. and Hanley, H. J. M., The viscosity and thermal conductivity coefficients of dilute nitrogen and oxygen. *J. Phys. Chem. Ref. Data*, 1974, **3**, 979–1018.
17. Jan, N., Large lattice random site percolation. *Physica A*, 1999, **266**, 72–75.